J|A|C|S ARTICLES

Published on Web 05/06/2009

Switchable Molecular Conductivity

Ke Wang,[†] Norma L. Rangel,[†,‡] Subrata Kundu,[†,§] Juan C. Sotelo,[‡] Roberto M. Tovar,[‡] Jorge M. Seminario,*[,†,‡,▽] and Hong Liang*[,†,§]

College of Engineering, Texas A&M University, College Station, Texas 77843-3123

Received February 13, 2009; E-mail: hliang@tamu.edu; jorge.seminario@chemail.tamu.edu

Abstract: We demonstrate the switchability of the molecular conductivity of a citrate. This was made possible through mechanical stretching of two conformers of such citrate capped on and linked between gold nanoparticles (AuNPs) self-assembled as a film. On the basis of experimental results, theoretical analysis was conducted using the density function theory and Green's function to study the electron flux in the backbone. We found that the molecular conductivity depended on the pathways of electrons that were controlled by the applied mechanical stress. Under stress, we could tune the conductivity up and down for as much as 10-fold. The mechanochemistry behind this phenomenon is an alternative branch of chemistry.

Introduction

Since the first report on electrical characteristics of single molecules, extensive efforts have been made to model electrical conduction on nanosized materials in order to explain transport mechanisms in small structures.[1] Adapted methods from solid-state physics were initially used to explain such a behavior with gross approximations using methodologies that were less insightful than common quantum chemistry calculations.[2] Those methods generally ignored chemistry. Some methods, such as the extended Hückel model, were used and claimed to yield good results.[3] The Hartree−Fock method and the local density approximations were applied, yet the chemical behavior at interfaces remained unknown.[4,5]

We have developed procedures to characterize and calculate, from first principles, the electrical characteristics of nanomaterials where the chemistry is the central focus of the calculation. In our method, the physics and/or extended features are brought through a Greens function approach (GENIP program).[6−8] As this procedure is fully ab initio, it is not limited to specific conduction regimes, which constraints empirical procedures based on phenomenological Hamiltonians. Our approach is to avoid problems related to the empirical rules of conductance[9] that can be used with chemically accurate methods with similar levels of theory for the continuous and discrete parts of the problem. It is expected that the final product is a fully ab initio procedure with chemical accuracy.

To experimentally control the pathway of electron movement, a mechanical force is believed to be a simple and effective method. It has been reported that a mechanical force can activate covalent bonds in polymers and guide reaction pathways of molecules.[10−12] We have recently found that a mechanical force can dominate the oxidation kinetics and dynamics of tantalum resulting in nonequilibrium oxides.[13,14] Here we apply a mechanical force to control the pathway of electrons. We used citrate-capped gold nanoparticles (AuNPs) as the model system. Results showed that we could switch the molecular conductivity of a self-assembled film made of such particles. This opens new avenues for development of single electronic devices of which molecular conductivity could be switched on and off and to a desired value.

Experimental Section

Reagents. Hydrogen tetrachloroaurate trihydrate ($HAuCl_4 \cdot 3H_2O$, 99.9%) and trisodium citrate dihydrate ($Na_3C_6H_5O_7 \cdot 2H_2O$, 99.99%) (Sigma-Aldrich) were used as reaction media for AuNPs. The deionized (DI) water was used for all synthesis. Citrate-capped AuNPs were synthesized by exploiting the well-known Turkevich method.[15]

Preparation of Au NP Film. Polyvinylidene fluoride (PVDF) was used as the substrate for the thin film preparation. PVDF

[†] Materials Science and Engineering.
[‡] Chemical Engineering.
[§] Mechanical Engineering.
[▽] Electrical Engineering.

(1) Seminario, J. M.; Cordova, L. E.; Derosa, P. A. *Proc. IEEE* **2003**, *91*, 1958–1975.
(2) Das, G. P.; Mark, J. E. *Polym. Bull.* **1988**, *19*, 469–476.
(3) Lindsay, D. M.; Wang, Y.; George, T. F. *J. Cluster Sci.* **1990**, *1*, 107–126.
(4) Yaliraki, S. N.; Roitberg, A. E.; Gonzalez, C.; Mujica, V.; Ratner, M. A. *J. Chem. Phys.* **1999**, *111*, 6997–7002.
(5) Hall, L. E.; Reimers, J. R.; Hush, N. S.; Silverbrook, K. *J. Chem. Phys.* **2000**, *112*, 1510–1521.
(6) Hong, S.; Jauregui, L. A.; Rangel, N. L.; Cao, H.; Day, S.; Norton, M. L.; Sinitskii, A. S.; Seminario, J. M. *J. Chem. Phys.* **2008**, *128* (1−4), 201103.
(7) Yan, L.; Bautista, E. J.; Seminario, J. M. *Nanotechnology* **2007**, *18*, 485701.
(8) Sotelo, J. C.; Yan, L.; Wang, M.; Seminario, J. M. *Phys. Rev. A* **2007**, *75*, 022511.
(9) Seminario, J. M. *J. Phys. B* **2007**, *40*, F275−F276.
(10) Beyer, M. K.; Clausen-Schaumann, H. *Chem. Rev.* **2005**, *105*, 2921–2948.
(11) Grandbois, M.; Beyer, M.; Rief, M.; Clausen-Schaumann, H.; Gaub, H. E. *Science* **1999**, *283*, 1727–1730.
(12) Schmidt, S. W.; Beyer, M. K.; Clausen-Schaumann, H. *J. Am. Chem. Soc.* **2008**, *130*, 3664–3668.
(13) Kar, P.; Wang, K.; Liang, H. *Electrochem. Solid-State Lett.* **2008**, *11*, 13–17.
(14) Kar, P.; Wang, K.; Liang, H. *Electrochim. Acta* **2008**, *53*, 5084–5091.
(15) Turkevich, J.; Stevenson, P. C.; Hillier, J. *Discuss. Faraday Soc.* **1951**, *11*, 55–75.

 © 2009 American Chemical Society

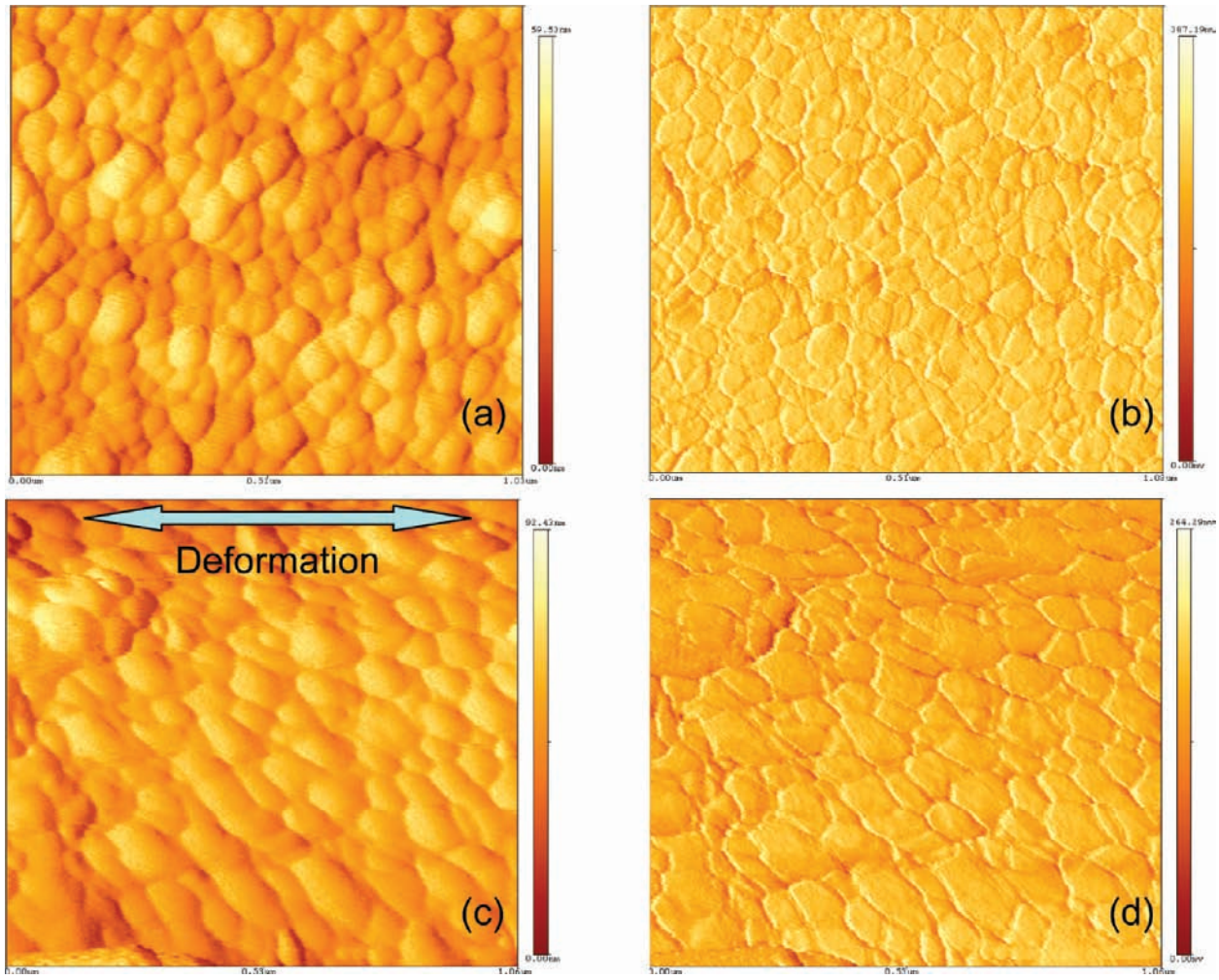

Figure 1. Noncontact mode AFM images of self-assembled AuNP film. (a) Surface morphology/without deformation; (b) phase image/without deformation; (c) surface morphology/with deformation; and (d) phase image/with deformation.

substrates were cleaned thoroughly in acetone with sonication for 20 min and functionalized with poly(allylamine hydochloride) (PAH, 0.1% by weight).[16] The functionalized substrates were immersed in the AuNP solution for about 30 min and dried in a vacuum chamber. After the first monolayer was deposited, the surface was visible as light pink. Subsequent layers were deposited by repeated alternate immersion in AuNP solution and drying. Finally, a golden metallic luster was obtained after eight depositions.

Instruments. Topographic and phase images were obtained using an atomic force microscope (Nano-R, Pacific Nanotechnology Inc.) in noncontact mode. Standard silicon nitride cantilevers (Nano World) were used. The transmission electron microscopy (TEM) analysis was carried out using a JEOL JEM-2010. The X-ray photoelectron spectroscopy (XPS) analysis was conducted using a Kratos Axis Ultra Imaging X-ray photoelectron spectrometer with monochromatic Al Kα line (1486.7 eV) (Materials Characterization Facility, Texas A&M University). The UV−visible (UV−vis) absorption spectra were recorded in a Hitachi (Model U-4100) UV−vis−NIR spectrophotometer. The conductivity measurement was performed by a TTP4 cryogenic probe station (Desert Cryogenics, LLC.) and a HP 4145 semiconductor parameter analyzer. The applied current sweeps in a staircase manner according to the input parameters, and the voltage is measured at the end of each current step. Measurements were taken at room temperature. To investigate how the resistance of AuNP film responds to longitudinal deformation, we attached the substrate (thickness, $T = 52\ \mu$m) with AuNP film to a cylindrical supporter with a diameter (D) of 1 cm. Since $D \gg T$, the resulting strain (ε) can be calculated from the relation $\varepsilon \cong (D/T + 1)^{-1}$, which is 0.5%.

Computational Details

We optimized the geometry of the molecular junctions and determined their structural stability with the B3PW91 fully nonlocal functional[17−20] using the 6-31G(d)[21,22] basis set for C, H, and O and the effective core potential and basis set LANL2DZ[23−25] for Au level as implemented in the Gaussian 03 program.[26] The current through the junction was computed via density functional theory (DFT) and Green's function implementation of an extended Landau formalism (GENIP).[27−29]

Results and Discussions

Morphological Characteristics. Atomic force microscopic (AFM) images of the film over a 1 μm × 1 μm area are shown in Figure 1a and b for the as-prepared film and Figure 1c and d for the mechanically stretched film (strain = 0.5%). Surface morphologies are given in Figure 1a and c, and phase images (for sharper characterization of grain boundaries) in Figure 1b and d. The AuNPs are seen aligning in the direction of stretch. This indicates that the applied force does indeed affect the AuNPs on the surface. In sample preparation, we self-assembled AuNPs on top of a PVDF substrate. During fabrication of the PVDF, the material was polled by stretching along the diagonal

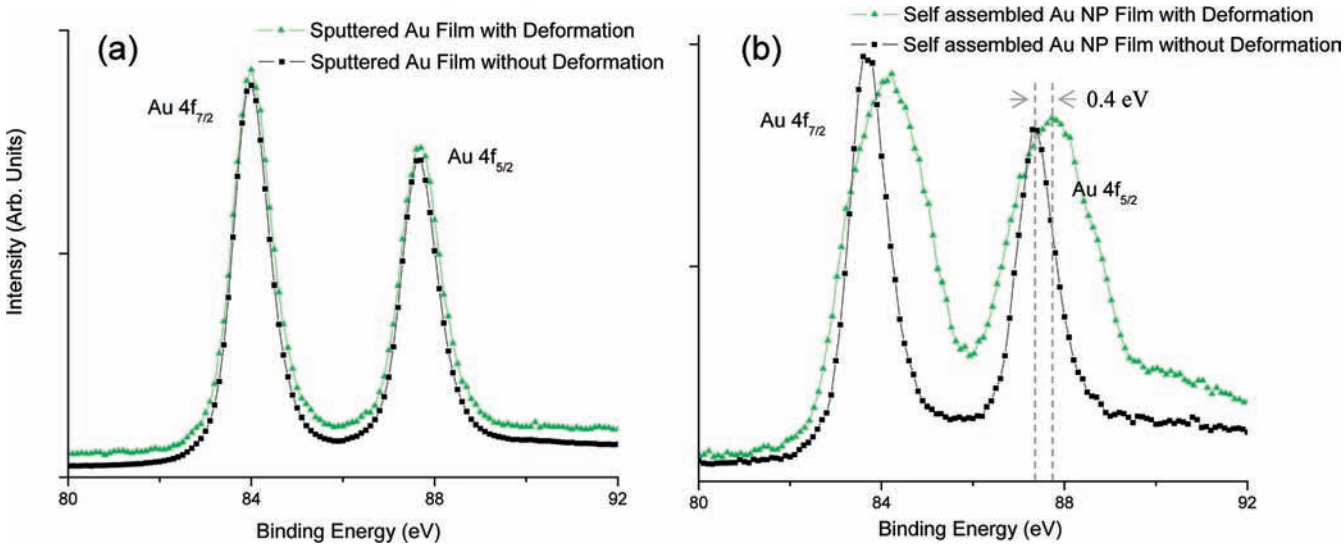

Figure 2. Au 4f XPS spectra of (a) sputtered Au film, and (b) self-assembled AuNP film.

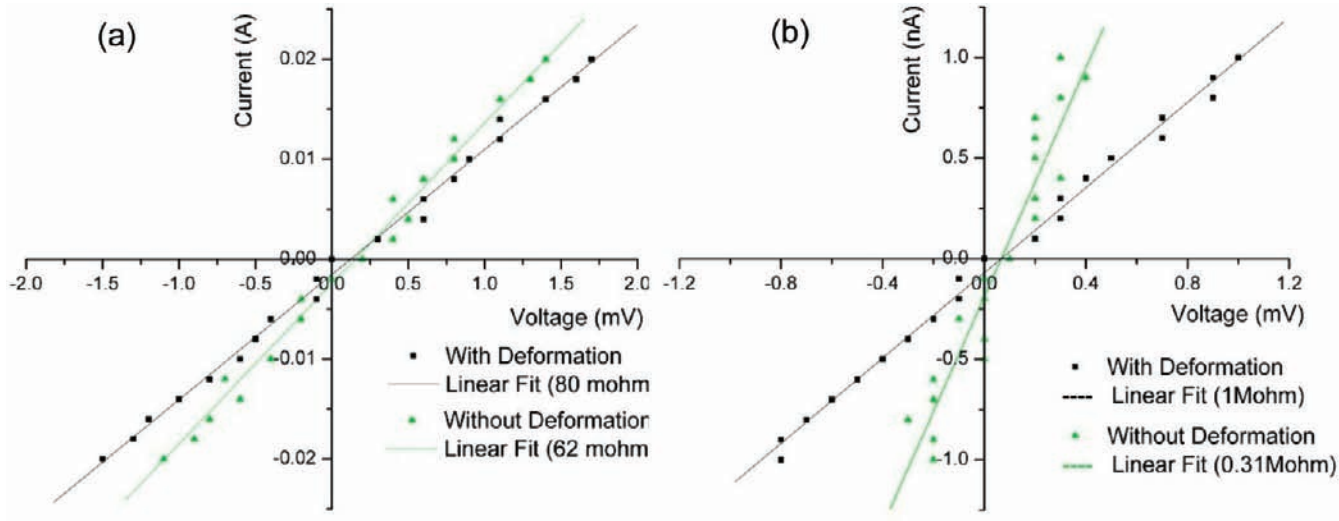

Figure 3. *I*−*V* measurements of sputtered Au film and self-assembled AuNP film. (a) Sputtered Au film with and without deformation and (b) self-assembled AuNP film with and without deformation.

Table 1. List of Energies, Relative Energies, HOMO and LUMO Energies, and HOMO−LUMO Gaps (HLG) for the Standalone and Extended Citrates

molecule	energy (Ha)	relative energy (kcal/mol)	HOMO (eV)	LUMO (eV)	HLG (eV)
Citrate-1	−757.729473	3.60	−8.54	−5.90	2.64
Citrate-2	−757.735219	0.00	−8.49	−5.90	2.59
Citrate-1 Au_2	−1028.609268	0.00	−7.46	−6.07	1.39
Citrate-2 Au_2	−1028.597795	7.20	−7.18	−4.90	2.29

direction at 850 °C for more than 8 hrs. In our experiments, a stress was applied in the horizontal direction. The deformation of PVDF was visible along the polling direction (diagonal). The deformation of AuNPs was apparent along the diagonal direction. It is expected that the space between particles increases under the stress. As seen in Figure 1c and d, the gaps between adjacent particles are larger in the stretched sample (Figure 1d) than the as-prepared one (Figure 1b). The effect of stress is further confirmed by surface roughness measurement as shown in Figure 1a and 1c. The roughness increases from ∼7.6 nm for the as-prepared film to ∼13.4 nm for the stretched film. The above results relate to deformations that have been observed on the film surface.

The TEM results are given in Figures S1 and S2 (Supporting Information). The images clearly show that AuNPs are encapsulated by citrate molecules. The physical connection between citrate molecules between individual AuNPs was identified. Details are given in the Supporting Information.

Spectroscopic Analysis. As we have seen, the AuNP film responds to stress with structural modifications such as adjusting interparticle separations. This leads to stretching of the citrate molecules capping the AuNPs. As a result, the electronic properties of the film will be affected. We have used XPS to explore such effects under longitudinal elongation (strain = 0.5%). As shown in Figure 2b, the electron binding energy (BE) Au $4f_{7/2}$ is shifted for 0.4 eV compared

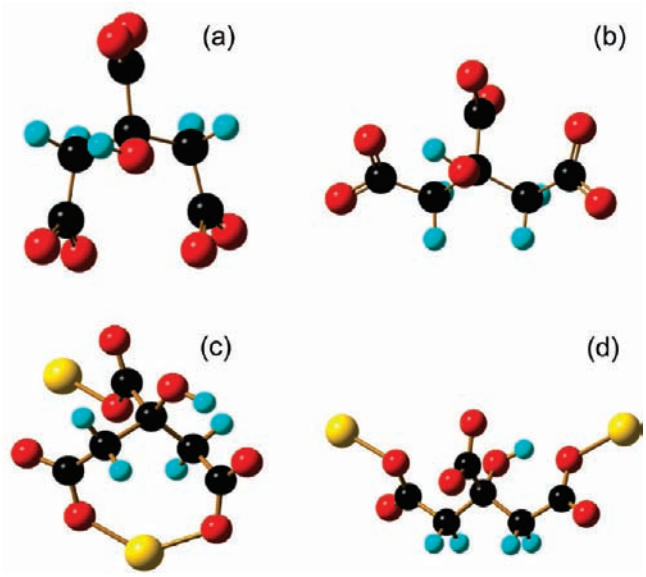

Figure 4. Two conformers of 2-hydroxypropane-1,2,3-tricarboxylate. Standalone Citrate-1 (a) and Citrate-2 (b); extended (with one-gold-atom electrodes) Citrate-1 (c) and Citrate-2 (d).

with the unstretched film. The peak's full width at half-maximum (fwhm) was increased by 90%. This suggests that the chemical environment of Au atoms in self-assembled AuNP film was altered by stress, where the shift in BE is an indicative of the presence of Au oxide.[30] Unlike the AuNP film, the Au 4f peaks of a sputtered Au film were not affected by stress, as shown in Figure 2a. This indicates that the self-assembled film is more sensitive to the external deformation than the sputtered one.

The UV−vis absorption spectra were done on the AuNP films before and after applied stress (Figure S3 in the Supporting Information). A small red-shift for the surface plasmon band of AuNPs was observed due to the applied stress. The large red-shift due to the cross-linking of AuNPs was reported.[31]

Effects of Stress on the Conductivity. To examine the electronic transport properties of the AuNP film, a current−voltage ($I-V$) curve was measured at room temperature. In the elongation direction (Figure 3b), the average resistance of the film was increased from 0.31 to 1 MΩ under stress, a 223% increase. In contrast, only a moderate increase (from 62 to 80 mΩ) was found in the sputtered Au film (Figure 3a), i.e., a 29% increase.

Theoretical Analysis of Conductivity. Our results showed that the conductivity of a self-assembled AuNP film was dominated by the encapsulated molecules under stress. In order to understand this further, we conducted ab initio calculation.

Two citrate conformers with the lowest energies (Table 1) are considered to model the bridge-molecule between two AuNPs before and after the application of an external force, as labeled Citrate-1 (Figure 4a) and Citrate-2 (Figure 4b). Their configurations, when inserted in the junctions (namely, extended with one-atom gold electrodes), are shown in Figure 4c and d. When a force is exerted on the film, it is likely that the average interparticle distance between the particles increases (as suggested by Figure 1d). We choose the shortest of the molecular bridges (as measured by the distance between gold atoms), Citrate-1 (6.2 Å), as the representative between NPs before film stretching; and the longest, Citrate-2

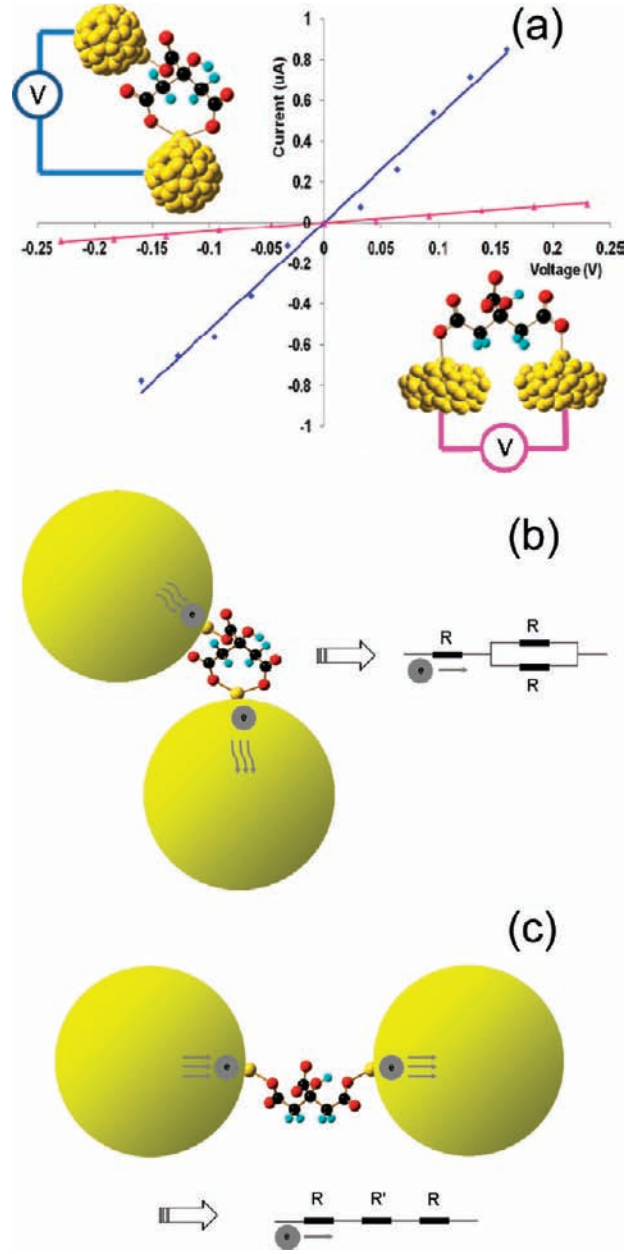

Figure 5. Electron path characteristics. (a) Simulated $I-V$ curve; (b) simplified model for electron path without stress; and (c) simplified model for electron path under stress.

(8.93 Å), as that after. We assume that they are the representative bridges along the conductivity percolation paths in our model film before and after elongation, respectively.

There are two reasons for such a choice. First, Citrate-1-Au_2 is more stable than Citrate-2-Au_2 by 7.20 kcal/mol (Table 1). It is therefore a more likely configuration to be present in the relaxed (unstretched) film. Second, the length difference between each citrate is 2.73 Å, such that using the average diameter of AuNPs (70 nm), the stress-induced transition from Citrate-1 to the Citrate-2 structure is ∼0.4%, close to the calculated strain (0.5%).

The transformation from a Citrate-1 junction to a Citrate-2 will affect the electrical properties of our model film. This is apparent from the ∼65% increase in the transport barrier as calculated value of the junction's HOMO−LUMO gap

(Table 1). In such, the presence of a Citrate-2 junction will decrease the conductivity of the film. This is in fact what we observe in the calculated $I-V$ characteristics of the junctions (Figure 5a). The resistance of the Citrate-1 junction (sample without deformation) is 0.2 MΩ (blue line and top left of Figure 5a); that of the Citrate-2 junction (sample with deformation) is 2 MΩ (pink line and bottom right of Figure 5a). These are compared with the resistances obtained from the measured $I-V$ characteristics of the self-assembled-AuNP film, with and without deformation (Figure 3b). The film has a resistance of 0.31 MΩ before deformation and 1 MΩ after. Therefore, both in model and experimental results (Figures 5a and 3b), an increase of the resistivity is found after elongation. Nevertheless, they have different increasing ratio (change of resistance/initial resistance). For simulation this ratio is 10 and for experiment about 3. This is to be expected due to the simplicity of the interface structures used in our model film, i.e., a binary set. A slightly more realistic interface would consider a mixture of both junctions, whereby there are more Citrate-1 junctions at the interface before deformation and more Citrate-2 junctions after, resulting in the reduction of the increase ratio. This behavior can be further illustrated using a simplified model, as shown in Figure 5b and d. In Figure 5b, two large balls represent the AuNPs. A molecule of citrate is attached at each end. When a voltage is applied, the electron goes through in a simplified circuit as shown. In Figure 5c, likewise, under a stress, the electron goes through a different circuit as shown in Figure 5c. The change of paths is only possible due to an applied stress.

Conclusions

We investigated the response of electron flux of a self-assembled AuNP film to a mechanical force. Under stress, the electron pathway underwent a transition between conformers of encapsulating citrate molecules. The stress-induced transition of conductivity was confirmed both in experiments and simulation. This indicates that it is possible to design single-electron devices of which molecular conductivity could be switched on and off and to a desired value.

Acknowledgment. J.M.S. acknowledges the support of DTRA/ARO. H.L. thanks the support of NSF 0535578. Authors wish to acknowledge the support provided by the Materials Characterization Facility (MCF) and the Microscopy and Imaging Center (MIC) at Texas A&M University for XPS, UV−vis, and TEM analysis.

Supporting Information Available: TEM images of Au NPs, UV−vis spectra, and complete ref 26. This material is available free of charge via the Internet at http://pubs.acs.org.

JA901156X

(16) Muller, K.; Quinn, J. F.; Johnston, A. P. R.; Becker, M.; Greiner, A.; Caruso, F. *Chem. Mater.* **2006**, *18*, 2397–2403.
(17) Frisch, M. J.; Pople, J. A.; Binkley, J. S. *J. Chem. Phys.* **1984**, *80*, 3265.
(18) Becke, A. D. *J. Chem. Phys.* **1993**, *98*, 1372–1377.
(19) Perdew, J. P.; Wang, Y. *Phys. Rev. B* **1992**, *45*, 13244–13249.
(20) Perdew, J. P.; Chevary, J. A.; Vosko, S. H.; Jackson, K. A.; Pederson, M. R.; Singh, D. J.; Fiolhais, C. *Phys. Rev. B* **1992**, *46*, 6671–6687.
(21) Hehre, W. J.; Ditchfield, R.; Pople, J. A. *J. Chem. Phys.* **1972**, *56*, 2257–2261.
(22) Hariharan, P. C.; Pople, J. A. *Chem. Phys. Lett.* **1972**, *16*, 217.
(23) Wadt, W. R.; Hay, P. J. *J. Chem. Phys.* **1985**, *82*, 284–298.
(24) Hay, P. J.; Wadt, W. R. *J. Chem. Phys.* **1985**, *82*, 299–310.
(25) Hay, P. J.; Wadt, W. R. *J. Chem. Phys.* **1985**, *82*, 270–283.
(26) Frisch, M. J. *Gaussian 03*; Gaussian, Inc.: Pittsburgh, PA, 2003.
(27) Derosa, P. A.; Seminario, J. M. *J. Phys. Chem. B* **2001**, *105*, 471–481.
(28) Seminario, J. M.; Zacarias, A. G.; Derosa, P. A. *J. Chem. Phys.* **2002**, *116*, 1671–1683.
(29) Sotelo, J. C.; Yan, L.; Wang, M.; Seminario, J. M. *Phys. Rev. B* **2007**, *75*, 022511.
(30) Maye, M. M.; Y. Lin, J. L.; Engelhard, M. H.; Hepel, M.; Zhong, C. J. *Langmuir* **2003**, *19*, 125–131.
(31) Chatterjee, A.; Oh, D. J.; Kim, K. M.; Youk, K. S.; Ahn, K. H. *Chem. Asian J.* **2008**, *3*, 1962–1967.